MIT Libraries | DSpace@MIT

MIT Open Access Articles

Analysis of Thermal Diodes Enabled by Junctions of Phase Change Materials

The MIT Faculty has made this article openly available. ***Please share*** how this access benefits you. Your story matters.

Citation: Cottrill, Anton L., and Michael S. Strano. "Analysis of Thermal Diodes Enabled by Junctions of Phase Change Materials." Adv. Energy Mater. 5, no. 23 (September 10, 2015): n/a–n/a.

As Published: http://dx.doi.org/10.1002/aenm.201500921

Publisher: Wiley Blackwell

Persistent URL: http://hdl.handle.net/1721.1/102318

Version: Author's final manuscript: final author's manuscript post peer review, without publisher's formatting or copy editing

Terms of use: Creative Commons Attribution-Noncommercial-Share Alike

Massachusetts Institute of Technology

DOI: 10.1002/aenm.201500921

Article type: Full Paper

Analysis of Thermal Diodes Enabled by Junctions of Phase Change Materials

*Anton L. Cottrill and Michael S. Strano**

A. L. Cottrill, Prof. M. S. Strano

Department of Chemical Engineering

Massachusetts Institute of Technology

Cambridge, MA 02139, USA

E-mail: strano@mit.edu

Keywords: thermal rectification, thermal diodes, phase change materials

Materials designed to undergo a phase transition at a prescribed temperature have been advanced as elements for controlling thermal flux. Such phase change materials can be used as components of reversible thermal diodes, or materials that favor heat flux in a preferred direction; however, a thorough mathematical analysis of such diodes is thus far absent from the literature. Herein, it is shown mathematically that the interface of a phase change material with a phase invariant one can function as a simple thermal diode. Design equations are derived for such phase change diodes, solving for the limits where the transition temperature falls within or outside of the temperature gradient across the device. Criteria are derived analytically for the choice of thermal conductivity of the invariant phase to maximize the rectification ratio. Finally, the model is applied to several experimental systems in the literature, providing bounds on observed performance. This model should aid in the development of materials capable of controlling heat flux.

1. Introduction

A thermal rectifier, the thermal analog to the electrical diode, is a device characterized by a preferential direction for heat flow.[1] The degree of thermal rectification is typically quantified under steady state conditions. It is equal to the ratio of the magnitudes of forward heat flux and reverse heat flux under forward and reverse temperature bias conditions of identical magnitudes, respectively.

We can consider a 1-D system in contact with a hot temperature boundary condition, T_H, on one side and a cold temperature boundary condition, T_C, on the opposing side. This temperature bias will provide a steady state heat flux, q_+, in the direction from T_H to T_C. A reversal of the temperature bias, while maintaining its magnitude, yields the steady state heat flux, q_-, in the opposite direction. In the case of a thermal rectifying device, the magnitudes of these two heat fluxes will be unequal, and their ratio is termed the rectification ratio, Q.

An asymmetrical thermal conductance was first recognized experimentally at the interface of copper and copper oxide in 1936 by Starr *et al*.[2] The phenomenon of thermal rectification has paved the way for the field of phononics[1] via the development of thermal transistors,[3-6] thermal logic circuits,[7] and thermal memory.[8] Furthermore, thermal diodes have a vast array of applications in the fields of nano-scale and micro-scale heat management.[9,10] Various strategies have been implemented for experimentally demonstrating a thermal rectifier. Researchers have applied electronic principles, such as semiconductor technology, towards thermal diode design.[2,11-12] In addition, the incorporation of geometric asymmetries into nano-structured, micro-structured, and bulk devices has yielded promising results.[13-17] The manipulation of contact areas between interfaces, due to thermal warping, has also proven successful as a thermal diode design.[10]

A promising method for developing a device with thermal rectification is to introduce a non-linear element, such as a material with a temperature-dependent thermal conductivity, into the system. Furthermore, in order to break the symmetry imposed by the boundary conditions, an additional

element, linear or non-linear, should be interfaced with the non-linear element, introducing a space dependency for thermal conductivity. Mathematically, this corresponds to transforming the system's steady state energy balance from a non-linear autonomous differential equation to a non-linear non-autonomous differential equation. For example, a device composed of a material with a temperature-dependent thermal conductivity (non-linear element) interfaced with a material with a temperature-independent thermal conductivity (linear element) would satisfy these constraints. Ideally, it is envisioned that the two interfaced materials would have opposing trends in thermal conductivity as a function of temperature. Experimental observations of thermal rectification due to interfaces between materials of different thermal conductivity temperature dependencies date to the 1970s.[18-20] Current examples of thermal rectifiers that incorporate this design have been demonstrated experimentally by Takeuchi *et al.* and Kobayashi *et al*., achieving rectification ratios up to 1.43.[15, 21-22]

Several strides have been made towards the numerical and analytical modeling of these non-linear systems at steady state. M. Peyrard analyzed such a system with basic continuum laws of heat conduction.[23] He proposed modelling the steady state thermal diode system with a non-linear non-autonomous differential equation. The system's rectification ratio can then be calculated through self-consistent iteration, provided data for the materials' thermal conductivities as a function of temperature are available. It should be noted that Kobayashi *et al*. used this numerical approach to calculate the theoretically predicted rectification ratios of their system, which agreed well with their experimental values.[15, 21] Hu *et al*. simulated such a thermal diode system by performing Hamiltonian mechanics calculations of coupled φ^4 and Frenkel-Kontorova lattices, in order to simulate the opposing trends of thermal conductivity with respect to temperature.[24] On a similar note, researchers have also modeled coupled segments with different thermal conductivity temperature dependencies with two-dimensional asymmetrical Ising models.[25] C. Dames developed an analytical model for this two-segment system by approximating the thermal conductivities with power law expressions and solving the resulting

differential equations with perturbation analysis. The analysis agreed well with experimental results in literature and provided more insight towards the design of such devices.[26]

Employing phase change materials to obtain a variation in physical properties with respect to temperature is an emerging avenue for designing thermal diodes.[27-30] Recently, a thermal diode was developed with a two-segment design consisting of nitinol and graphite. Nitinol, a nickel titanium alloy, undergoes a change in thermal conductivity as the material transitions between the austenite and martensite crystal structures. Researchers have reported experimental thermal rectification ratios up to 1.47 for such a device.[27] A concept for a phase-change radiative thermal diode has also been proposed.[28] A two-segment device consisting of poly(*N*-isopropylacrylamide) (PNIPAM), a phase-changing polymer, and polydimethylsiloxane (PDMS) has also been demonstrated to show thermal rectification. Below the lower-critical-solution-temperature (LCST) of the PNIPAM polymer, water is immobilized throughout the polymer. However, above the LCST the water exits the polymer, which changes its configuration and reduces its size. In this case, the thermal conductivity of the PNIPAM does not necessarily alter. Rather, the effective thermal conductivity of the composite system changes, yielding thermal rectification when interfaced with PDMS, which has a temperature-independent thermal conductivity. A simple model based on a smooth step change in effective thermal resistance with respect to temperature for the PNIPAM was proposed by the researchers to model the system. This model was analyzed numerically, and it yielded thermal rectification estimates close to the experimental values obtained.[29]

The intent of this paper is to further the understanding of thermal rectifying devices that are based on changes in thermal conductivity due to phase transitions. A simple, analytical model based on continuum laws of heat conduction at steady state will be proposed for understanding the relevant thermal resistances for device optimization. Furthermore, this model will be applied to experimental data existing in the literature and compared to numerical calculations based on the method outlined by

M. Peyrard.[23] Finally, this model will be used to elucidate optimal design strategies for other potential phase change thermal diodes based on data present in the literature.

2. Problem Statement

Consider the junction of two 1-D materials A and B, of lengths L_A and L_B, respectively, and with material B possessing a first-order phase transition at temperature T^* from phase B_1 at a temperature below T^* to phase B_2 at a temperature above T^*. For simplicity, we refer to A as the invariant material, having no phase transition for all T. The temperature-dependent thermal conductivity of material A is $k_A(T)$ while B has thermal conductivity $k_{B,1}(T)$ for phase 1 and $k_{B,2}(T)$ for phase 2. We analyze the case where this material is temperature-controlled, such that the external boundary of A is maintained isothermally at T_2 while the external boundary of B is at T_1, and the heat flux in the system reaches a stationary state. **Figure 1a** depicts the physical schematic of the junction of materials A and B. We first assume that $T_1 < T^* < T_2$, and in the case of Figure 1a, this implies that phase B_1 is the low temperature phase, transitioning to phase B_2 upon heating the system above T^*. We therefore anticipate a phase boundary at a distance δ from the external B interface as shown in Figure 1a, which varies with T_1 and T_2, the lengths of each material, L_A and L_B, and the thermal properties of the composite system.

Fourier's Law for material A and for each phase of material B at steady state is as follows:

$$\frac{\partial}{\partial x}\left(k_A(T)\frac{\partial T}{\partial x}\right) = 0 \quad (1)$$

$$\frac{\partial}{\partial x}\left(k_{B,1}(T)\frac{\partial T}{\partial x}\right) = 0 \quad (2)$$

$$\frac{\partial}{\partial x}\left(k_{B,2}(T)\frac{\partial T}{\partial x}\right) = 0 \quad (3)$$

The heat flux through the 1-D system must be invariant at steady state, such that:

$$k_A(T)\frac{\partial T}{\partial x} = k_{B,1}(T)\frac{\partial T}{\partial x} = k_{B,2}(T)\frac{\partial T}{\partial x} = -q \quad (4)$$

With $x = 0$ taken as the external B interface, the boundary conditions become:

$$T(x = 0) = T_1 \quad (5)$$

$$T(x = \delta) = T^* \quad (6)$$

$$T(x = L_B) = T_i \quad (7)$$

$$T(x = L_A + L_B) = T_2 \quad (8)$$

where T_i is the interfacial temperature between materials A and B. Equal thermal flux boundary conditions existing at the interface between the two phases of material B and the interface between materials A and B are also applied.

In order to quantify the magnitude of thermal rectification, the reversal of the temperature boundary conditions shown in Figure 1a needs to be considered. A reversal of these temperature boundary conditions yields Figure 1b. The ratio of the magnitudes of the thermal fluxes between the two systems described in Figure 1 yields the thermal rectification ratio for this system. Mathematically predicting the magnitude of thermal rectification can be approached analytically or numerically, as presented below.

2.1. Case I: Constant Thermal Conductivities and {δ: 0 < δ < L_B}

The type of diode of primary consideration in this work is one enabled by the change of phase of B. Such a phase change diode can operate if $T_1 < T^* < T_2$. For Case I, we further restrict the analysis to conditions such that {δ: 0 < δ < L_B}. We consider the case of constant thermal conductivity for simplicity, noting that it applies in general for a diode operating about the temperature T^* with a

relatively small-applied temperature gradient. Non-constant thermal conductivities can be treated in a manner described below in Case III.

In this case, the linear temperature profiles for domains A, B_1, and B_2 for the system illustrated in Figure 1a are:

$$T_A(x) = \left(\frac{T_2 - T_i}{L_A}\right)(x - L_B) + T_i \tag{9}$$

$$T_{B,1}(x) = \left(\frac{T^* - T_1}{\delta}\right)x + T_1 \tag{10}$$

$$T_{B,2}(x) = \left(\frac{T_i - T^*}{L_B - \delta}\right)(x - \delta) + T^* \tag{11}$$

The interfacial temperature T_i is a function of thermophysical properties and applied temperatures:

$$T_i = -\left(\frac{k_{B,2}(T_2 - T^*) + k_{B,1}(T^* - T_1)}{k_A L_B + k_{B,2} L_A}\right)L_A + T_2 \tag{12}$$

while the phase boundary in B appears at:

$$\delta_{1-2} = \frac{k_{B,1}}{k_A}\frac{(T^* - T_1)(k_A L_B + k_{B,2} L_A)}{k_{B,2}(T_2 - T^*) + k_{B,1}(T^* - T_1)} \tag{13}$$

where the subscript 1-2 indicates the direction of the imposed temperature gradient, as evidenced by the locations of T_1 and T_2.

The magnitude of the steady flux through this system is then:

$$|q_{1-2}| = k_A\left(\frac{k_{B,2}(T_2 - T^*) + k_{B,1}(T^* - T_1)}{k_A L_B + k_{B,2} L_A}\right) \tag{14}$$

where the subscript 1-2 indicates the direction of the imposed temperature gradient, as evidenced by the locations of T_1 and T_2.

If we consider the flux in the opposing direction, should T_1 be applied instead to the $x = L_A + L_B$ boundary, and T_2 applied to $x = 0$ boundary, we note that the ordering of the phases necessarily changes to that of Figure 1b. Specifically, phase B_2, and not phase B_1, becomes the external boundary for the B domain. From symmetry, we can set $T_1 \rightarrow T_2$ and $k_{B,1} \rightarrow k_{B,2}$ to find the opposing flux under this condition:

$$|q_{2-1}| = k_A \left(\frac{k_{B,1}(T^* - T_1) + k_{B,2}(T_2 - T^*)}{k_A L_B + k_{B,1} L_A} \right) \tag{15}$$

Interestingly, the rectification ratio becomes:

$$Q = \frac{|q_{1-2}|}{|q_{2-1}|} = \frac{k_A L_B + k_{B,1} L_A}{k_A L_B + k_{B,2} L_A} \tag{16}$$

The model proposed above is valid under the following circumstances:

$$0 < \delta_{1-2} < L_B \quad and \quad 0 < \delta_{2-1} < L_B \tag{17}$$

Application of these inequalities yields constraints for the validity of the model:

$$\frac{k_A}{k_{B,2}} > \frac{L_A}{L_B} \frac{(T^* - T_2)}{(T_1 - T^*)} \qquad (\text{from } \delta_{2-1}) \tag{18}$$

$$\frac{k_A}{k_{B,1}} > \frac{L_A}{L_B} \frac{(T^* - T_1)}{(T_2 - T^*)} \qquad (\text{from } \delta_{1-2}) \tag{19}$$

Therefore, when the thermophysical properties and applied temperature gradient satisfy Equation (18) and (19), Equation (16) can be used to predict the thermal rectification ratio for the system. For systems in which the applied temperature gradient and thermophysical properties yield $\delta \geq L_B$, indicating the absence of a phase boundary, a different model needs to be considered. The parameter δ was originally defined as the distance from the external B interface at which a phase boundary occurs. Physically, a phase boundary cannot exist at $\delta \geq L_B$ because this is in the domain of material A. This

constraint should then be physically interpreted as the position in the composite material at which the temperature is T^*.

2.2. Case II: Constant Thermal Conductivities and {δ: δ ≥ L_B}

Under certain conditions, the phase change material will exist as a single phase under both sets of temperature boundary conditions (1-2 and 2-1). In other words, for certain systems and boundary conditions, there will be no phase change boundaries within the phase transition material. Figure 2 qualitatively illustrates the thermal conductivity distributions of such a system for a general set of temperature boundary conditions. This system can be analyzed as a combination of linear systems, which have a change in thermal conductivity of the phase change material upon reversal of the temperature bias. A steady state solution for this linear system can be obtained by applying the appropriate temperature boundary conditions at the ends of the two-segment system and equal temperature and equal thermal flux constraints at the interface. Equation (20) and (21) are the temperature profiles for the phase change material and the invariant material, respectively, under the temperature bias shown in Figure 2a.

$$T_B(x) = \frac{(T_i - T_1)}{L_B} x + T_1 \tag{20}$$

$$T_A(x) = \frac{(T_2 - T_i)}{L_A} (x - L_B) + T_i \tag{21}$$

Again, the interfacial temperature T_i is a function of thermophysical properties and applied temperatures:

$$T_i = \frac{k_A L_B T_2 + k_{B,1} L_A T_1}{k_{B,1} L_A + k_A L_B} \tag{22}$$

The magnitude of the steady state flux though the system is then:

$$|q_{1-2}| = \frac{k_A k_{B,1}(T_2 - T_1)}{k_A L_B + k_{B,1} L_A} \tag{23}$$

where the subscript 1-2 indicates the direction of the imposed temperature gradient, as evidenced by the locations of T_1 and T_2.

If we consider the flux in the opposing direction, should T_1 be applied instead to the $x = L_A + L_B$ boundary, and T_2 applied to $x = 0$ boundary, we note that the ordering of the phases necessarily changes to that of Figure 2b. From symmetry, we can set $T_1 \rightarrow T_2$ and $k_{B,1} \rightarrow k_{B,2}$ to find the opposing flux:

$$|q_{2-1}| = \frac{k_A k_{B,2}(T_2 - T_1)}{k_A L_B + k_{B,2} L_A} \tag{24}$$

The rectification ratio is then given by Equation (25), which is a result supported by recent analytical work performed by Zhang *et al*.[30]

$$Q = \frac{|q_{1-2}|}{|q_{2-1}|} = \frac{k_{B,1}(k_{B,2} L_A + k_A L_B)}{k_{B,2}(k_{B,1} L_A + k_A L_B)} \tag{25}$$

Again, Equation (25) can only be applied to determine the thermal rectification of the system if $\delta \geq L_B$ for both sets of boundary conditions. In other words, the following inequalities must be satisfied in order to apply this model:

$$\frac{k_A}{k_{B,2}} \leq \frac{L_A}{L_B} \frac{(T^* - T_2)}{(T_1 - T^*)} \qquad \text{(from } \delta_{2-1}\text{)} \tag{26}$$

$$\frac{k_A}{k_{B,1}} \leq \frac{L_A}{L_B} \frac{(T^* - T_1)}{(T_2 - T^*)} \qquad \text{(from } \delta_{1-2}\text{)} \tag{27}$$

It can be envisioned that certain thermophysical properties and temperature boundary conditions will exist for a device such that for one set of boundary conditions the temperature profile will be appropriately modeled by Equation (9-13), while the reverse boundary conditions will be appropriately

modeled with Equation (20-22). Under these circumstances, neither Equation (16) nor Equation (25) is valid to predict the thermal rectification ratio for the system. The thermal rectification ratio for these systems can be calculated by mixing the models proposed in Case I and Case II.

For $\frac{k_A}{k_{B,2}} \leq \frac{L_A}{L_B}\frac{(T^*-T_2)}{(T_1-T^*)}$ and $\frac{k_A}{k_{B,1}} > \frac{L_A}{L_B}\frac{(T^*-T_1)}{(T_2-T^*)}$

$$Q = \frac{k_{B,1}(T^*-T_1)+k_{B,2}(T_2-T^*)}{k_{B,2}(T_2-T_1)} \tag{28}$$

For $\frac{k_A}{k_{B,2}} > \frac{L_A}{L_B}\frac{(T^*-T_2)}{(T_1-T^*)}$ and $\frac{k_A}{k_{B,1}} \leq \frac{L_A}{L_B}\frac{(T^*-T_1)}{(T_2-T^*)}$

$$Q = \frac{k_{B,1}(T^*-T_1)+k_{B,2}(T_2-T^*)}{k_{B,1}(T_2-T_1)} \tag{29}$$

Table 1 summarizes the results for the estimation of the thermal rectification ratio as a function of the thermophysical system properties and the applied temperature gradient.

2.3. Case III: Non-Constant Thermal Conductivities

The system illustrated in Figure 1 has constant thermal conductivities as a function of temperature for material A and the two phases of material B. This system can be modeled as a combination of linear conducting elements. However, if a temperature-dependent thermal conductivity is present for material A or either of the phases for material B, numerical computation is required. Additionally, one can exclude from consideration the operation of the device in Figure 1 under conditions such that material B exists only in phase B_1 ($T_1, T_2 < T^*$) or exists only in phase B_2 ($T_1, T_2 > T^*$), since thermal rectification does not occur. However, if non-constant thermal conductivities are present, thermal rectification can exist in these limits. This is the basis for the thermal diodes demonstrated experimentally by Kobayashi *et al*. and Takeuchi *et al*.[21-22] These devices need to be modeled numerically, unless the temperature dependencies of the thermal conductivity can be approximated

with power laws – a case in which the system can be modeled analytically by the method developed by C. Dames.[26] The method for numerically modeling such systems is described below, as developed by M. Peyrard.[23]

For a system at steady state, with a space-dependent, temperature-dependent, and isotropic thermal conductivity, the energy balance is as follows:

$$\nabla \cdot (k(T(\boldsymbol{x}), \boldsymbol{x})\, \nabla T(x)) = 0 \tag{30}$$

where k refers to the thermal conductivity, T refers to the temperature, and $\boldsymbol{x}$ refers to the position vector of the system. For a 1-D system Equation (30) can be simplified:

$$J = k(T(x), x)\frac{dT}{dx} \tag{31}$$

where J is the thermal flux due to conduction. The numerical analysis proposed by M. Peyrard employs an alternative form of Equation (31) in order to solve for the thermal rectification and temperature profile of a system:[23]

$$T(x) - T(0) = \int_0^x \frac{J}{k(T(x'), x')}\, dx' \tag{32}$$

To numerically solve for the thermal rectification of a system using Equation (32), the thermal conductivity of the segments as a function of temperature must be known. An iterative, self-consistent approach is then taken to solve the equation. An initial guess for the temperature profile within the system is used in combination with the boundary conditions and the thermal conductivity data to solve for the conductive heat flux, J, of the system. Values for the temperature profile, $T(x)$, can then be generated and compared with the initial guess for the temperature profile. A non-linear optimization method can be used to minimize the difference between the calculated and guessed temperature

profiles. This was the strategy used by Kobayashi *et al*. to compare their experimental rectification ratios to their theoretical calculations.[21]

2.4. Optimization of a Phase Change Thermal Diode:

For device optimization, there are three independent parameters which can be varied for a given $k_{B,1}$ & $k_{B,2}$:

$$\tilde{L} = \frac{L_A}{L_B} \; and \;\; k_A \; and \; \tilde{T} = \frac{T^* - T_1}{T_2 - T_1}$$

In order to analyze the design of such a device, let us first assume a system with $k_{B,1} > k_{B,2}$ and investigate the effect of the three independent parameters $(\tilde{L}, k_A, \tilde{T})$ on the system's thermal rectification performance. Figure 3a shows a piecewise volcano plot for device design at fixed $\tilde{L} = 1$ and $\tilde{T} = 0.1$ values, for a certain system with $k_{B,1} = 50$ W m^{-1} K^{-1} and $k_{B,2} = 1$ W m^{-1} K^{-1}. It is apparent that a maximum in rectification is approached as the two outer regions (Case I and Case II) converge towards a mixed model region, which is characterized by a Case I model in one temperature bias and a Case II model in the other temperature bias. Furthermore, it is clear that the device will yield an optimum thermal rectification ratio when the design is such that the transition temperature occurs at the interface between the phase change material B and the invariant material A under both temperature biases. This occurs at an ideal temperature bias, where the region modeled with Case I and the region modeled with Case II converges, such that the mixed model region collapses, as can be seen in Figure 3b.

Mathematically, the convergence of the Case I and Case II regions occurs when $\delta = L_B$ for both temperature biases. This is a stricter constraint than that for Case II, which was presented in Equation (26) and (27), because it indicates that the device is operating such that $T_i = T^*$. On the other hand, Equation (26) and (27) for Case II, only require that material B exists in a single phase and that T^* can

occur anywhere within material A. Applying this constraint to Equation (26) and (27) yields Equation (33), indicating that there is an ideal $\tilde{T}$ for device performance for a given $k_{B,1}$ and $k_{B,2}$.

$$\tilde{T}_{id} = \frac{\sqrt{k_{B,2}}}{\sqrt{k_{B,2}}+\sqrt{k_{B,1}}} \tag{33}$$

where $\tilde{T}_{id}$ refers to the ideal $\tilde{T}$ for device performance.

Application of this ideal temperature bias, $\tilde{T}_{id}$, to Equation (26) or (27) yields Equation (34), which provides the necessary relationship between k_A and $\tilde{L}$ for optimum device performance. In addition, application of Equation (33) to Equation (28) yields Equation (35), which provides the maximum thermal rectification ratio that can be obtained by the system. Equation (34) and (35) is supported by recent analytical work performed by Zhang *et al.*[30]

$$k_A = \tilde{L}\sqrt{k_{B,1}k_{B,2}} \tag{34}$$

$$Q_{max} = \frac{\sqrt{k_{B,1}k_{B,2}}+k_{B,2}}{\sqrt{k_{B,1}k_{B,2}}+k_{B,1}} \tag{35}$$

where Q_{max} refers to the maximum thermal rectification ratio that can be achieved by the system when operated at the ideal temperature bias, $\tilde{T}_{id}$, with the system's thermal resistances also satisfying Equation (34).

For the model system described in Figure 3, the application of Equation (33) and (35) indicates that $\tilde{T}_{id}$ and Q_{max} are 0.12 and 7.1, respectively. This thermal rectification will be achieved at the given $\tilde{T}_{id}$ provided that the thermal resistances within the system satisfy Equation (34). Figure 4 shows the evolution of a contour plot for the thermal rectification ratio as $\tilde{T}$ is varied for this particular system. It is apparent that as $\tilde{T}_{id}$ is approached from above and below, the mixed model region collapses and the

optimal rectification ratio enhances dramatically. In addition, the linear relationship between k_A and $\tilde{L}$ is shown in the contour plots.

3. Application to Experimental Phase Change Materials

A thermal diode based on the junction between the crystalline phase change material nitinol (B) and the invariant material graphite (A) was developed by Garcia *et al.*[27] For this system $k_{B,1}$ and $k_{B,2}$ would be defined by the crystal lattice structures of martensite (7.8 W m^{-1} K^{-1}) and austenite (17.3 W m^{-1} K^{-1}), respectively, for the nitinol phase change material (B). In addition, $\tilde{L} = 1$ and $T^* = 330\ K$, based on the reference data provided by Garcia *et al*. The invariant material (A), graphite, is assumed to have a temperature invariant thermal conductivity of 72.5 W m^{-1} K^{-1}, also based on reference data provided by the researchers. For their thermal rectification measurements, the researchers maintained $T_1 = 290\ K$ and varied T_2 up to 450 K. Based on the provided temperature boundary condition values, $\tilde{T}$ ranges can be calculated and the applicable models for certain temperature boundary conditions can be determined. Figure 5a shows a comparison of the experimental thermal rectification results from Garcia *et al*. with numerically and analytically derived thermal rectification ratios for the system. The numerically derived thermal rectification ratios were obtained according to the strategy outlined for Equation (32), using the thermal conductivity data provided by Garcia *et al*. for nitinol and graphite as functions of temperature. The thermal conductivity data provided by the researchers were fitted to a smooth function in order to numerically calculate the expected thermal rectification ratios. It should be noted that the temperature range for the experimental thermal conductivity values for nitinol reported by Garcia *et al.* is $280\ K < T < 380\ K$. Therefore, when $T_2 = 390\ K$ and $\Delta T = 100\ K$, the range of known thermal conductivity values for nitinol has been exceeded. In order to compare experimental data with the numerical and analytical models, it was assumed that above $T = 380\ K$ the thermal conductivity plateaued at the value for austenite. The analytical models applied to the system refer to

the Case I and Case II models, which were appropriately applied according to Table 1, depending on the applied temperature bias and the thermophysical properties of the system. The developed analytical models should only be applied to the experimental data with temperature biases enclosing the phase transition temperature. For that reason, analytically derived data points are not present as the temperature bias decreases in Figure 5a. It is apparent that the numerical and analytical calculations for the expected thermal rectification values are in agreement. In addition, the experimental thermal rectification values are in agreement with the models until $\Delta T = 100\,K$ is reached. However, at temperature biases $\Delta T > 100\,K$ – the range where we have extrapolated the thermal conductivity values for nitinol – the numerical and analytical models are no longer in agreement with the experimental thermal rectification values. We attribute this disagreement to the lack of experimental data for the thermal conductivity of the nitinol material above $T = 380\,K$.

A thermal diode based on a phase change polymer has been experimentally and conceptually discussed by Pallecchi *et al*.[29] The thermal diode consists of a PNIPAM-PDMS two-segment system, in which PNIPAM acts as the phase change material (B) and PDMS acts as an invariant material (A). Experimental thermal rectification values are not explicitly reported by Pallecchi *et al*. However, values for thermal fluxes under a variety of forward and reverse temperature biases are reported, refer to Figure 6a, which can be used to calculate experimental values for the thermal rectification of their system, as shown in Figure 6b. As previously mentioned, for application of the developed analytical models, it is necessary for the temperature biases to enclose the phase transition temperature. This accounts for the range of the experimental data provided in Figure 6a. The heat flux data for the forward and reverse temperature biases were fitted with linear regressions in order to calculate the experimental thermal rectification ratio as a function of the magnitude of the temperature bias, as shown in Figure 6b. Based on the thermal resistances and system dimensions provided by the researchers, the relevant values for modeling this system are: $k_{B,1} = 0.101$ W m^{-1} K^{-1}, $k_{B,2} = 0.396$ W

m^{-1} K^{-1}, $k_A = 0.101$ W m^{-1} K^{-1}, and $\tilde{L} = 1$. Using these system parameters, the device constructed by Pallecchi *et al.* can be modeled with the analytical equations that have been presented, as shown in Figure 6b. The experimental results provided by Pallecchi *et al.* validate the developed analytical models, as indicated by the convergence of the experimental thermal rectification ratios (black) to the maximum predicted by the analytical model (green). Furthermore, the agreement between the experimental data and the analytical model indicates the utility of this straightforward, algebraic model towards accurately predicting thermal rectification performance and towards the effective design of such thermal diodes.

The design strategy outlined in Equation (33-35) for attaining the maximum thermal rectification can be applied to the systems described by Garcia *et al.* and Pallecchi *et al.* Application of these equations yields the optimal temperature gradient and the maximum attainable thermal rectification ratio. For operation of the devices at the ideal temperature gradient, the performance of the system can be modeled as a function of the thermal conductivity of the invariant material (A), in order to determine the ideal material to couple to the phase change material. Therefore, we will consider the phase change materials (B) employed by Garcia *et al*. and Pallecchi *et al.*, but we will design for a more appropriate phase-invariant material (A), other than graphite and PDMS, respectively. Figure 7 presents the results of these simulations. It should also be noted that the length scales for the devices proposed by Garcia *et al.* and Pallecchi *et al.* could have been adjusted according to Equation (34), instead of selecting another phase invariant material. Properly tuning the thermal conductivities or system length scales yields maximum thermal rectification ratios of 1.49 and 1.98 for the systems described by Garcia *et al.* and Pallecchi *et al*., respectively. For the thermal diode system developed by Garcia *et al.*, this maximum thermal rectification ratio of 1.49 refers to the maximum thermal rectification ratio that can be attained within the window of operation constrained by the range of the experimental thermal

conductivity data – where the numerical and analytical models are in agreement with the experimental data.

The ability to tune electrical and thermal conductivity with liquid-solid phase transitions in percolated composite materials has been recently reported in literature.[31] For a system of suspended graphite flakes in hexadecane, the room temperature liquid-solid phase transition results in a step-like change in thermal conductivity. Factors of 3.2 were reported for thermal conductivity amplification. In addition, the thermal conductivity showed stable, cycling behavior. For a 1 vol% suspension of graphite flakes in hexadecane, the relevant thermal properties are: $k_{B,1} = 1.2$ W m^{-1} K^{-1} and $k_{B,2} = 0.4$ W m^{-1} K^{-1}. The ideal temperature gradient ($\tilde{T}$) for this system is 0.37 and the maximum achievable thermal rectification ratio is 1.73. Figure 7c provides insight towards the selection of the invariant material (A) to interface with the suspension such that optimal thermal rectification performance can be achieved.

4. Conclusion

In this work we have developed an analytical model based on continuum laws of heat conduction to describe thermal rectification in devices that incorporate phase transition materials. The analytical model can be used to understand the effects of the system's thermal resistances, as well as the applied temperature gradients, on the device's thermal rectification performance. For a given phase transition material (B), with a certain phase transition temperature (T^*), as well as characteristic thermal conductivities for each phase ($k_{B,1}$ $k_{B,2}$), we outline a procedure for designing a thermal rectifying device with optimal performance using this analytical model. The procedure involves properly tuning the thermal resistances of the phase change material (B) and the phase invariant material (A), in addition to properly selecting a thermal bias for operation.

The analytical model was applied to experimental data in literature for two thermal diodes, which incorporated phase change materials, developed by Garcia *et al.* and Pallecchi *et al*. The comparison

between the experimental data and the analytical predictions for the two thermal diode systems showed agreement. For the nitinol-graphite thermal diode system developed by Garcia *et al*., the analytical and numerical thermal rectification predictions were in agreement. Furthermore, the theoretical models, numerical and analytical, were in agreement with the experimental data reported by Garcia *et al.* until a temperature bias of $\Delta T = 100\ K$ was reached. Temperature biases $\Delta T > 100\ K$ exceeded the known range for the thermal conductivity of the nitinol material and account for the discrepancy between theory and experiment at larger temperature biases. Though thermal rectification ratios for the thermal diode system developed by Pallecchi *et al.* were not explicitly reported, the values were able to be calculated from reported thermal flux values as a function of temperature bias. The calculated, experimental thermal rectification ratios for the PNIPAM-PDMS thermal diode system from Pallecchi *et al.* were in strong agreement with the analytical model. The analytical model was also applied to optimize the design of the thermal diodes developed by Garcia *et al.* and Pallecchi *et al.* For the nitinol thermal diode system, in the range of known thermal conductivity, it was shown that the thermal rectification ratio could be significantly enhanced by choosing a phase invariant material to replace graphite. The same conclusion was demonstrated for the PNIPAM thermal diode system – choosing a phase invariant material to replace the PDMS could drastically increase the thermal rectification ratio. Lastly, the analytical model was applied to the optimal design of a thermal diode based on a known phase transition material, which undergoes a modulation of thermal conductivity during its phase transition. The composite material, exfoliated graphite in hexadecane, undergoes thermal conductivity modulation in response to effects on the percolation network for heat conduction due to crystallinity changes during the phase transition. The maximum thermal rectification for this system was predicted to be 1.73 by the analytical model.

Acknowledgements

The authors acknowledge the Air Force Office of Scientific Research (AFOSR), under award FA9550-09-1-0700, for their financial support regarding this project.

Received: ((will be filled in by the editorial staff))
Revised: ((will be filled in by the editorial staff))
Published online: ((will be filled in by the editorial staff))

References

[1] L. Wang, B. Li, *Phys. World* **2008**, *21*, 27.

[2] C. Starr, *Physics* **1936**, *7*, 15.

[3] B. Li, L. Wang, G. Casati, *Appl. Phys. Lett.* **2006**, *88*, 143501-1.

[4] J. Zhu, K. Hippalgaonkar, S. Shen, K. Wang, Y. Abate, S. Lee, J. Wu, X. Yin, A. Majumdar, X. Zhang, *Nano Lett.* **2014**, *14*, 4867.

[5] W. C. Lo, L. Wang, B. Li, *J. Phys. Soc. Japan* **2008**, *77*, No. 5.

[6] N. Yang, N. Li, L. Wang, B. Li, *Phys. Rev. B* **2007**, *76*, 020301-1.

[7] L. Wang, B. Li, *Phys. Rev. Lett.* **2007**, *99*, 177208-1.

[8] L. Wang, B. Li, *Phys. Rev. Lett.* **2008**, *101*, 267203-1.

[9] B. Li, J. Lan, L. Wang, *Phys. Rev. Lett.* **2005**, *95*, 104302-1.

[10] N. A. Roberts, D. G. Walker, *Int. J. Therm. Sci.* **2011**, *50*, 648.

[11] V. Kislitsyn, S. Pavliuk, R. Soltys, V. Lozovski, G. Strilchuk, *IEEE Trans. Electron Devices* **2014**, *61*, 548.

[12] R. Scheibner, M. König, D. Reuter, a D. Wieck, C. Gould, H. Buhmann, L. W. Molenkamp, *New J. Phys.* **2008**, *10*, 083016.

[13] C. W. Chang, D. Okawa, A. Majumdar, A. Zettl, *Science* **2006**, *314*, 1121.

[14] P. W. O'Callaghan, S. D. Probert, a Jones, *J. Phys. D. Appl. Phys.* **1970**, *3*, 1352.

[15] D. Sawaki, W. Kobayashi, Y. Moritomo, I. Terasaki, *Appl. Phys. Lett.* **2011**, *98*, 081915.

[16] M. Schmotz, J. Maier, E. Scheer, P. Leiderer, *New J. Phys.* **2011**, *13*, 113027.

[17] H. Tian, D. Xie, Y. Yang, T.-L. Ren, G. Zhang, Y.-F. Wang, C.-J. Zhou, P.-G. Peng, L.-G. Wang, L.-T. Liu, *Sci. Rep.* **2012**, *2*, 523.

[18] C. Marucha, J. Mucha, J. Rafałowicz, *Phys. status solidi* **1975**, *31*, 269.

[19] A. Jeżowski, J. Rafalowicz, *Phys. status solidi* **1978**, *47*, 229.

[20] K. Balcerek, T. Tyc, *Phys. status solidi* **1978**, *47*, K125.

[21] W. Kobayashi, Y. Teraoka, I. Terasaki, *Appl. Phys. Lett.* **2009**, *95*, 171905-1.

[22] T. Takeuchi, H. Goto, Y. Toyama, T. Itoh, M. Mikami, *J. Electron. Mater.* **2011**, *40*, 1129.

[23] M. Peyrard, *Europhys. Lett.* **2006**, *76*, 49.

[24] B. Hu, D. He, L. Yang, Y. Zhang, *Phys. Rev. E* **2006**, *74*, 060201-1.

[25] L. Wang, B. Li, *Phys. Rev. E* **2011**, *83*, 061128-1.

[26] C. Dames, *J. Heat Transfer* **2009**, *131*, 061301-1.

[27] K. I. Garcia-Garcia, J. Alvarez-Quintana, *Int. J. Therm. Sci.* **2014**, *81*, 76.

[28] P. Ben-Abdallah, S. A. Biehs, *Appl. Phys. Lett.* **2013**, *103*, 191907-1.

[29] E. Pallecchi, Z. Chen, G. E. Fernandes, Y. Wan, J. H. Kim, J. Xu, *Mater. Horiz.* **2015**, *2*, 125.

[30] T. Zhang, T. Luo, *Small*, **2015**, DOI: 10.1002/smll.201501127

[31] R. Zheng, J. Gao, J. Wang, G. Chen, *Nat. Commun.* **2011**, *2*, 289.

Figures:

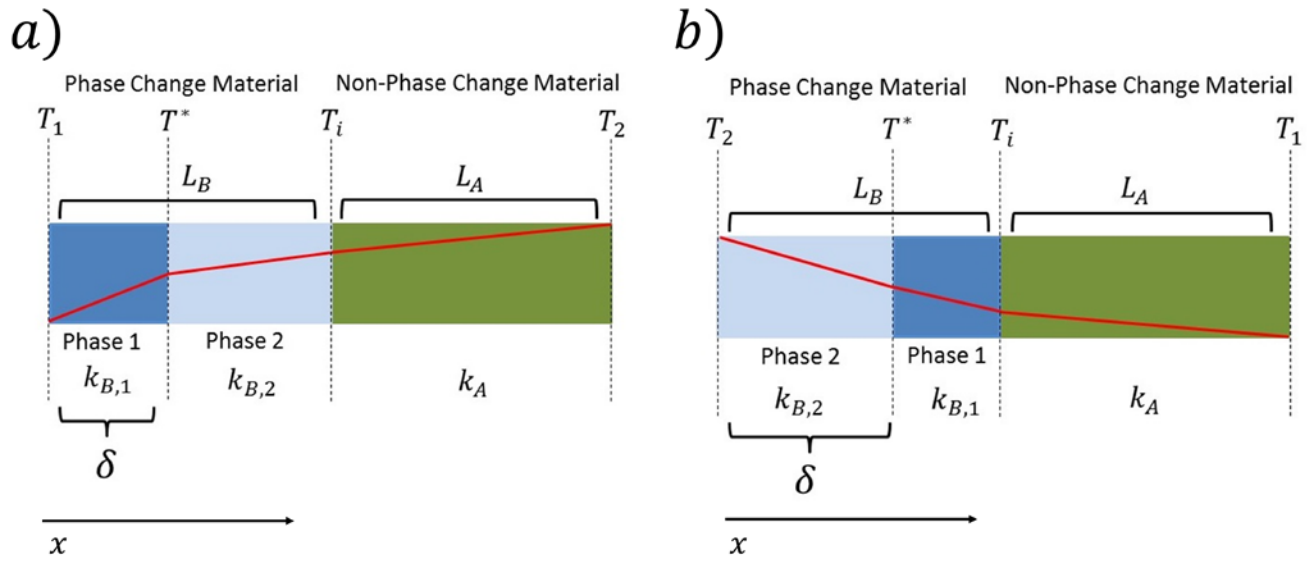

Figure 1. A schematic illustrating thermal rectification in a device consisting of a phase change material (B), with each phase characterized by a different thermal conductivity ($k_{B,1}, k_{B,2}$), interfaced with a phase invariant material (A) with thermal conductivity k_A. a) A representation of the temperature profile (red line) throughout the system when the external boundary of material B is below the transition temperature (T^*) and the external boundary of material A is above the transition temperature. The illustrated temperature profile is for the case where $k_{B,1}, k_{B,2}, \& k_A$ are constant with respect to temperature. b) A representation of the temperature profile (red line) throughout the system when the external boundary of material B is above the transition temperature and the external boundary of material A is below the transition temperature. The illustrated temperature profile is for the case where $k_{B,1}, k_{B,2}, and\ k_A$ are constant with respect to temperature. The spatial distribution of the phases within material B as the temperature boundary conditions are reversed should be noted.

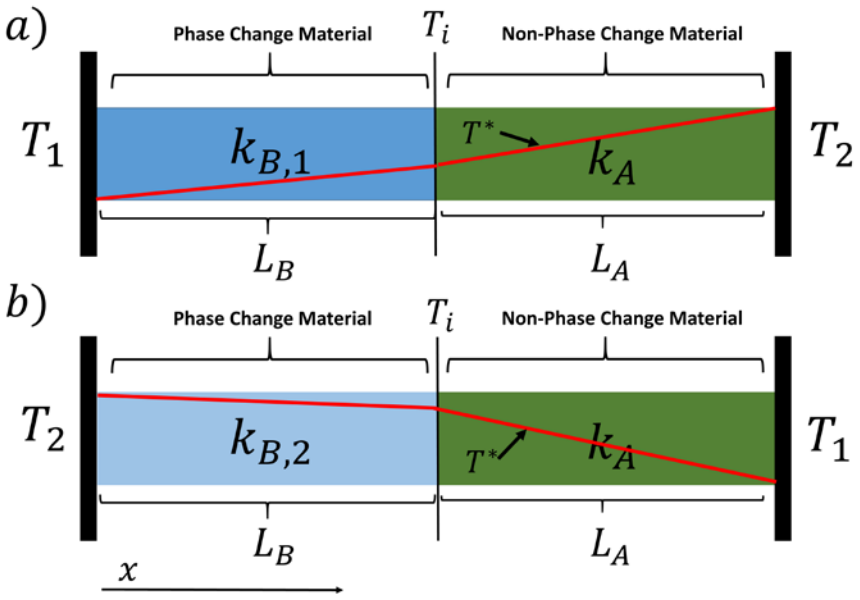

Figure 2. A schematic qualitatively illustrating thermal rectification in a device consisting of a phase change material (B), with each phase characterized by a different thermal conductivity ($k_{B,1}, k_{B,2}$), interfaced with a phase invariant material (A) with thermal conductivity k_A. a) A representation of the temperature profile (red line) throughout the system when the external boundary of material B is below the transition temperature (T^*) and the external boundary of material A is above the transition temperature. The illustrated temperature profile is for the case where $k_{B,1}$ & k_A are constant with respect to temperature. b) A representation of the temperature profile (red line) throughout the system when the external boundary of material B is above the transition temperature and the external boundary of material A is below the transition temperature. The illustrated temperature profile is for the case where $k_{B,2}$, & k_A are constant with respect to temperature. The distribution of the phases within material B as the temperature boundary conditions are reversed should be noted. Also, it can be noted that the transition temperature, T^*, occurs at a distance $x > L_B$.

Table 1. A chart summarizing the results for the estimation of the thermal rectification ratio for a given system consisting of a junction between an invariant material with constant thermal conductivity and a phase change material with constant thermal conductivities for each phase. $A > B$ & $C > D$ refers to a strictly Case I system. $A \leq B$ & $C \leq D$ refers to a strictly Case II system. The other two possibilities refer to a mixing of Case I and Case II.

$$A = \frac{k_A}{k_{B,2}} \qquad B = \frac{L_A}{L_B}\frac{(T^* - T_2)}{(T_1 - T^*)} \qquad C = \frac{k_A}{k_{B,1}} \qquad D = \frac{L_A}{L_B}\frac{(T^* - T_1)}{(T_2 - T^*)}$$

	$A > B$	$A \leq B$
$C > D$	$Q = \frac{k_A L_B + k_{B,1} L_A}{k_A L_B + k_{B,2} L_A}$	$Q = \frac{k_{B,1}(T^* - T_1) + k_{B,2}(T_2 - T^*)}{k_{B,2}(T_2 - T_1)}$
$C \leq D$	$Q = \frac{k_{B,1}(T^* - T_1) + k_{B,2}(T_2 - T^*)}{k_{B,1}(T_2 - T_1)}$	$Q = \frac{k_{B,1}(k_{B,2} L_A + k_A L_B)}{k_{B,2}(k_{B,1} L_A + k_A L_{B)}}$

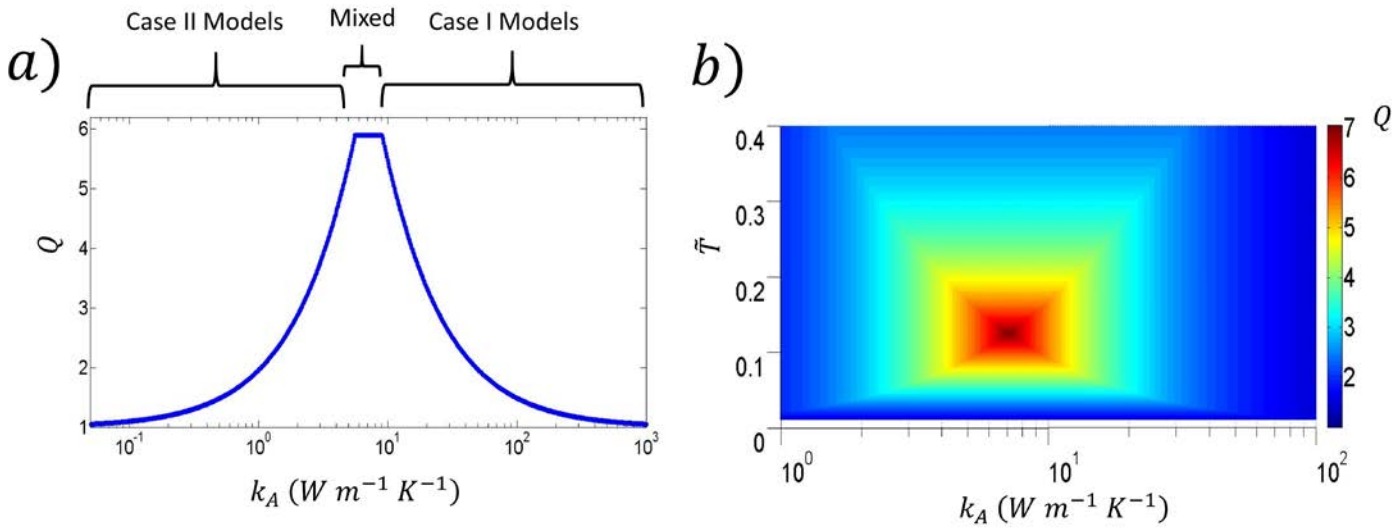

Figure 3. Plots illustrating the effects of the thermal conductivity of the invariant material (A) and the applied temperature bias towards the optimization of the thermal rectification performance for an assumed phase change material (B). a) A plot allowing optimal design of the thermal rectification ratio, Q, as a function of the thermal conductivity of the invariant material (A), k_A, for a fixed $\tilde{L} = 1$ & $\tilde{T} = 0.1$. $k_{B,1} = 50$ W m^{-1} K^{-1} & $k_{B,2} = 1$ W m^{-1} K^{-1} are also fixed as properties of the phase change material that is assumed. The plot is a piecewise function, where the relevant models used to derive specific regions are indicated by brackets. b) A contour plot demonstrating the convergence of Case I and Case II and the collapse of the mixed model region, yielding an

optimal thermal rectification performance, as an ideal temperature bias is approached. Q is plotted as a function of the thermal conductivity of the invariant material (A), k_A, and the applied temperature bias, $\tilde{T}$ at fixed $\tilde{L} = 1$. Again, $k_{B,1} = 50$ W m^{-1} K^{-1} & $k_{B,2} = 1$ W m^{-1} K^{-1} are also fixed as properties of the phase change material that is assumed.

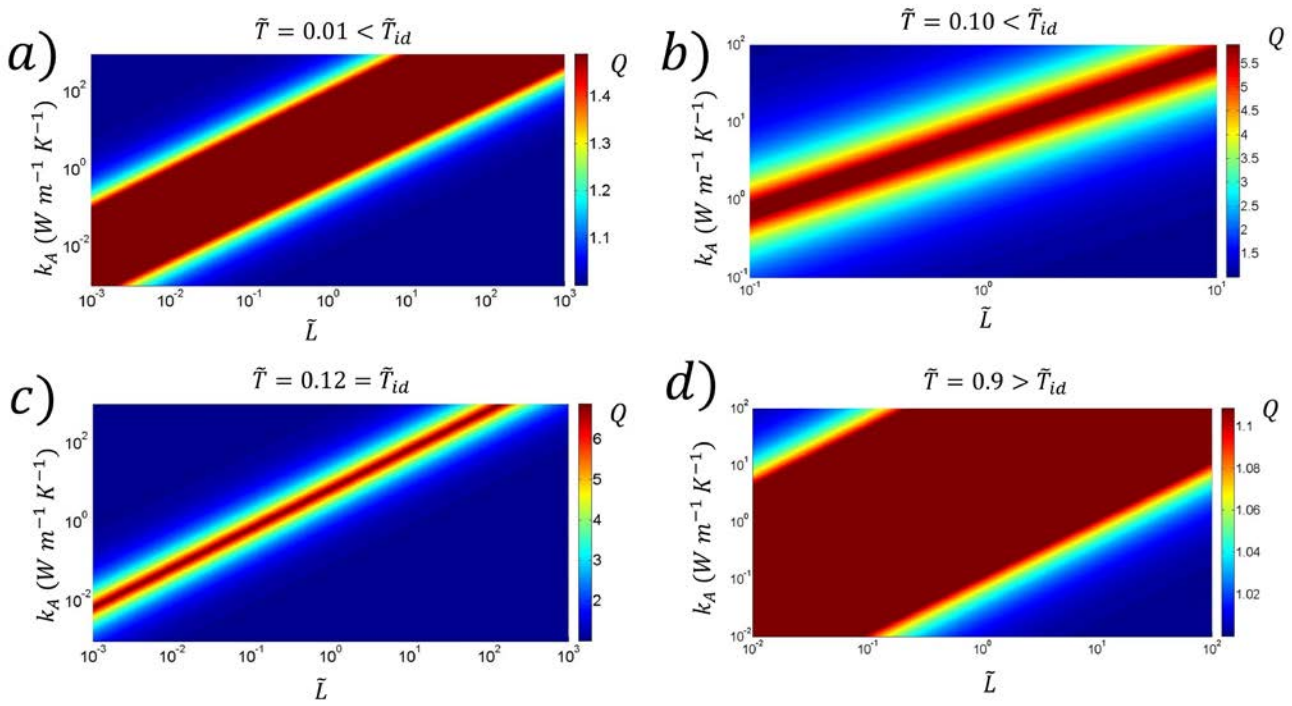

Figure 4. For a model system with $k_{B,1} = 50$ W m^{-1} K^{-1} & $k_{B,2} = 1$ W m^{-1} K^{-1}, the evolution of a contour plot for the thermal rectification ratio, Q, as a function of $\tilde{L}$ and k_A (W m^{-1} K^{-1}), as $\tilde{T}$ is varied around $\tilde{T}_{id}$ is shown. a) Contour plot for $\tilde{T} = 0.01$. b) Contour plot for $\tilde{T} = 0.10$. c) Contour plot for $\tilde{T} = \tilde{T}_{id} = 0.12$. d) Contour plot for $\tilde{T} = 0.9$.

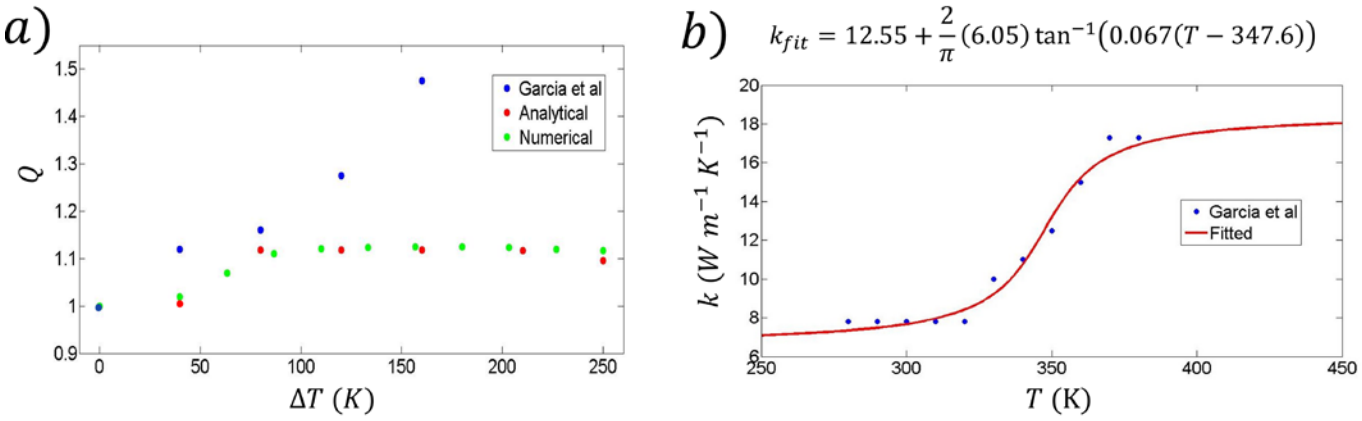

Figure 5. Comparison of the experimental thermal rectification ratios obtained by Garcia *et al.* for their nitinol phase change-based thermal diode to analytically and numerically predicted thermal rectification ratios for the system.[27]. The analytically calculated ratios were determined using the Case I and Case II models proposed above, while the numerically calculated ratios were determined using the strategy developed by M. Peyrard as in Equation (32).[23] a) Experimental (blue), analytical (red), and numerical (green) comparison for thermal rectification ratios as a function of temperature bias. b) A smooth function (red) fitted to the experimental thermal conductivity data (blue) from Garcia *et al.* for nitinol as a function of temperature.

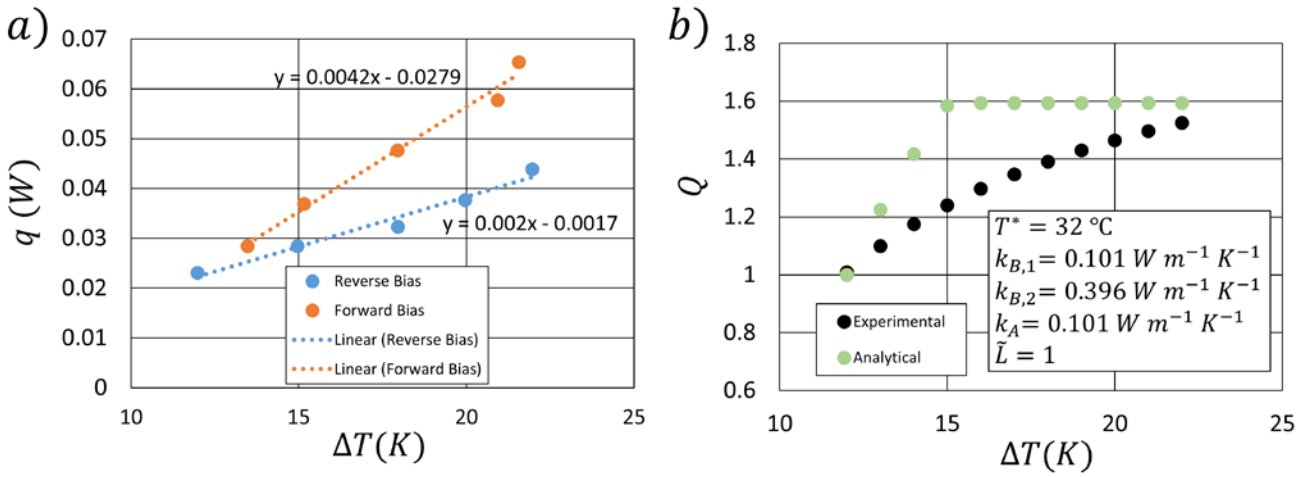

Figure 6. A comparison of the experimental thermal rectification data from Pallecchi *et al.* with the analytical thermal rectification predictions from the Case I and Case II models.[29] a) A plot of the heat flow, q, measured by Pallecchi *et al.* for their phase change-based thermal diode under a range of forward (orange) and reverse (blue) temperature biases, ΔT.[29] The data for each temperature bias were fitted with a linear regression. b) A

plot of the experimental and analytically predicted thermal rectification ratios, Q, as a function of the applied temperature bias, ΔT, for the phase change-based thermal diode developed by Pallecchi *et al*.[29] The experimental thermal rectification data (black), obtained from a ratio of the linear fits in a), is compared with the analytically predicted thermal rectification data (green). This diode incorporated a PNIPAM polymer as the phase change material (B) and a PDMS polymer as the phase invariant material (A). The relevant thermophysical parameters reported by the researchers, and used to model the system, are reported within the figure. The analytical thermal rectification values were generated according to the strategy outlined in Table 1, and they show significant agreement with the experimental values.

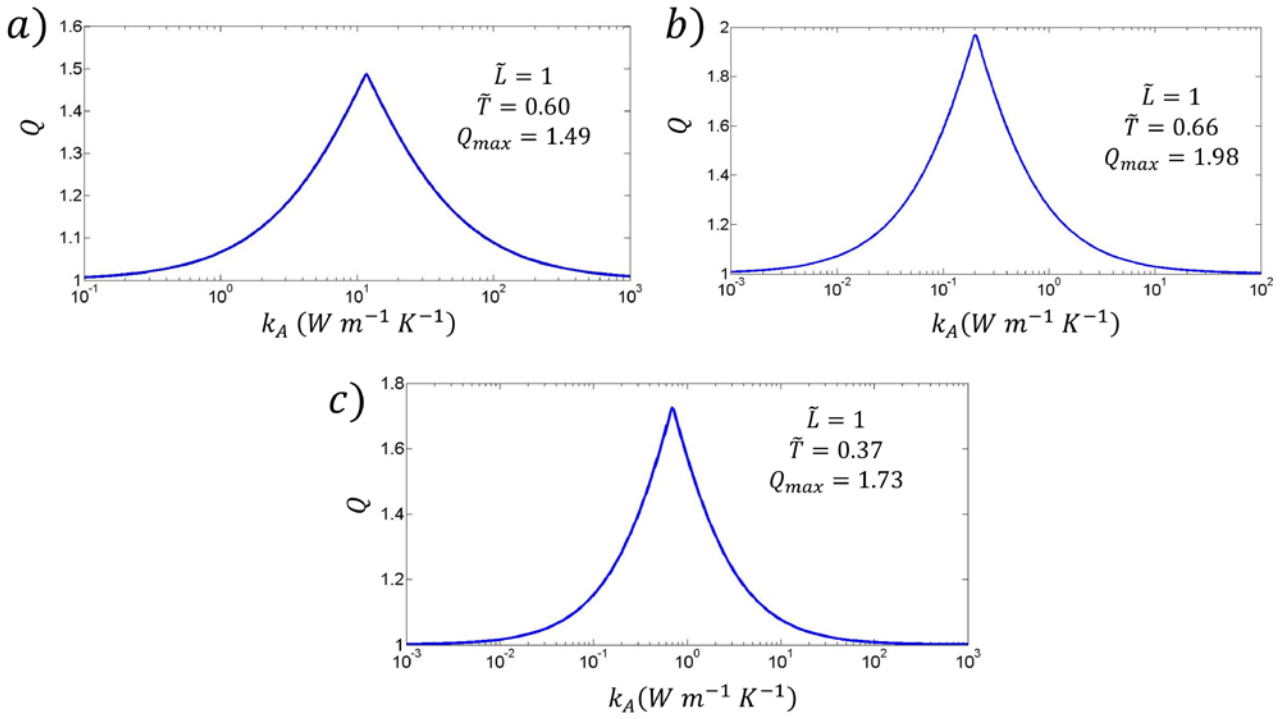

Figure 7. Optimization design plots for two phase change-based thermal diodes discussed in literature and an additional phase change material with thermal conductivity modulation that has yet to be incorporated into a thermal diode. a) Design plot for the nitinol-based thermal diode developed by Garcia *et al*.[27] The thermal rectification ratio, Q, as a function of the thermal conductivity, k_A, of the invariant material (A) is plotted for $\tilde{T} = \tilde{T}_{id} = 0.60$ and $\tilde{L} = 1$. b) Design plot for the PNIPAM-based thermal diode developed by Pallecchi *et al*.[29] The thermal rectification ratio, Q, as a function of the thermal conductivity, k_A, of the invariant material (A) is

plotted for $\tilde{T} = \tilde{T}_{id} = 0.66$ and $\tilde{L} = 1$. c) Design plot for a thermal diode based on liquid-solid phase transitions in a suspension of graphite flakes in hexadecane.[31] The thermal rectification ratio, Q, as a function of the thermal conductivity, k_A, of the invariant material (A) is plotted for $\tilde{T} = \tilde{T}_{id} = 0.37$ and $\tilde{L} = 1$.

Table of Contents:

Phase change materials can be used to construct thermal diodes. It is shown mathematically that the interface of such materials with a phase invariant material can function as a thermal diode. Criteria are derived analytically for the choice of thermal conductivity of the invariant phase to maximize the thermal rectification, and the model is applied to experimental systems in the literature.

Keyword: thermal diodes

Anton L. Cottrill, Michael S. Strano*

Analysis of Thermal Diodes Enabled by Junctions of Phase Change Materials